



Trade Science Inc.

Materials Science

An Indian Journal

Full Paper

MSAIJ, 8(1), 2012 [25-33]

Preparation, structure, thermal and dielectric properties of polyamide-montmorillonite nanocomposites

Nilufer Kivılcım, Turgay Seçkin*

Inonu University, Chemistry Department, 44280 Malatya (TURKEY)

E-mail : turgay.seckin@inonu.edu.tr

Received: 8th June, 2011 ; Accepted: 8th July, 2011

ABSTRACT

Polyamide-montmorillonite nanocomposites were prepared from solution of polyamide and the organo modified-montmorillonite (OM-MMT) using *N*-methyl-2-pyrrolidone as a solvent. The reactive organoclay was formed by using hexadecylpyridinium chloride (HPC) as a swelling agent for silicate layers of montmorillonite. The swelling process was carried out through ion exchange reaction between the end group of hexadecylpyridinium chloride salt and the sodium ion in montmorillonite. This irreversible swelling monitored by measuring the cation exchange capacity (CEC) of the montmorillonite solutions. Dispersion of the modified clay in the polyamide (kevlar) matrix resulted in nanostructured material containing intercalated polymer between the silicate layers. The Polyamide-montmorillonite nanocomposites films (PA-MMT) characterized by FTIR, SEM and x-ray were exfoliated nanocomposites at low MMT content (<1 wt.%) and partially exfoliated nanocomposites at high MMT content (containing aggregates of MMT). The clay content significantly influences thermal behavior of the nanocomposite films, such as glass transition and decomposition temperatures of polyamide-montmorillonite nanocomposites. The glass transition temperatures of the nanocomposites were higher than that of the original polyamide. The dielectric properties of the PA-clay nanocomposites were studied in detail. The results displayed that the dielectric constants decreased with the increase of the clay content and the films showed relatively low dielectric constant when the clay content was over 1 wt% compared to pure polyamide.

© 2012 Trade Science Inc. - INDIA

KEYWORDS

Polyamide;
Montmorillonite;
Nanocomposites;
Dielectric properties.

INTRODUCTION

Polyamides are large volume plastics widely used for structural and packaging applications. Their market spread is continuously growing due to their properties such as chemical and mechanical resistance, good bar-

rier properties to gases, clarity, printability, etc. The ultimate properties of end products are, of course, heavily dependent on the chemical structure of polyamide and on the process used to produce the manufactured articles^[1-3] and can be further increased using nanoparticles as additives to enhance the polymer performance. At

Full Paper

this regard, over last decade scientific research has paid great attention to polyamide/layered silicate nanocomposites because, compared to the unmodified resin, these systems provide enhanced performance properties such as improved tensile strength and moduli, decreased thermal expansion coefficient, decreased gas permeability, increased swelling resistance, enhanced ion conductivity, reduced flammability, etc^[4-7].

Polymer/layered silicate nanocomposites have become an important class of polymeric nanocomposites since they exhibit dramatic enhancement in barrier, thermal and mechanical properties^[8-10] even at very low silicate contents. It is well known that these properties are strongly affected by the affinity between the matrix and the clay, the degree of clay exfoliation, the dispersion and the orientation of clay particles throughout the thermoplastic matrix^[11]. Clay is a type of layered silicates. The most commonly used clay in the preparation of PA-clay nanocomposites is montmorillonite (MMT). It is about 100–218 nm in length and 1 nm in thickness. Montmorillonite is also called phlo-silicate with one octahedral Al_2O_3 sheet between two tetrahedral SiO_2 sheets^[12]. It can be intercalated or exfoliated in a polymer matrix to form the nanocomposite. In comparison to pure PA, recent studies in PA-clay nanocomposites exhibit improvements in thermal, mechanical, gas barrier properties as well as water absorption retardant behavior^[13-18]. Nonetheless, few publications to date have been reported on the dielectric properties at a fixed frequency and the dynamic mechanical properties of PA films^[19].

Polymer/layered silicate nanocomposites are prepared by various methods, such as melt intercalation, solvent intercalation and in situ intercalated monomer polymerization^[20-24]. But it is necessary to improve the dispersion ability of clay in the organic solvents or polymer matrix. Therefore, the silicate layer is generally modified by organic cations via ion exchange reactions. The new cation which has larger volume compare to Na^+ allows polymer easily access to the inter space between the layers^[25-27].

This article reports on polyamide-clay nanocomposite (PA-MMT) materials, consisting of *p*-phenylene diamine (PD) and terephthalic acid (TA), polyamide and layered montmorillonite (MMT) clay, that were successfully prepared by solution dispersion

technique. The as-synthesized PA-MMT nanocomposites were subsequently characterized by FTIR spectroscopy, X-ray diffraction (XRD), transmission electron microscopy (TEM) and scanning electron microscopy (SEM). The dielectric and thermal properties of the PA-clay nanocomposite films were studied in detail.

EXPERIMENTAL

Materials

Chemicals of high purity were obtained from various commercial sources, which consisted of *p*-phenylene diamine (PD; Aldrich), triphenyl phosphite (Aldrich), pyridine (merck), LiCl (Acros), terephthalic acid (TA, Acros), hexadecylpyridinium chloride (HPC; Aldrich) and *N*-methyl-2-pyrrolidone (NMP; Aldrich). NMP was purified by distillation under reduced pressure over calcium hydride and stored over 4 Å molecular sieves. Other organic solvents were purified by vacuum distillation. The other reagents were used as received.

Measurements

The samples were characterized by X-ray diffraction (XRD) for the crystal structure, average particle size and the concentration of impurity compounds present. Rigaku Rad B-Dmax II powder X-ray diffractometer was used for X-ray diffraction patterns of these samples. The 2θ values were taken from 20° to 110° with a step size of 0.04° using Cu $K\alpha$ radiation (λ value of 2.2897 Å). The dried samples were dusted on to plates with low background. A small quantity of 30(\pm 2) mg spread over 5 cm^2 area used to minimize error in peak location and also the broadening of peaks due to thickness of the sample is reduced. This data illustrate the crystal structure of the particles and also provides the inter-planar space, d . The broadening of the peak was related to the average diameter (L) of the particle according to Scherrer's formula, i.e. $L = 0.9\lambda / \Delta \cos \theta$ where λ is X-ray wavelength, Δ is line broadening measured at half-height and θ is Bragg angle of the particles.

Infrared spectra were recorded as KBr pellets in the range 4000 - 400 cm^{-1} on an ATI UNICAM systems 2000 Fourier transform spectrometer. Differential scanning calorimetry (DSC), differential thermal analy-

sis (DTA) and thermogravimetry (TG) were performed with Shimadzu DSC-60, DTA-50 and TGA-50 thermal analyzers, respectively.

Chemical composition analysis by EDAX was performed with an EDAX; Röntec xflash detector analyzer associated to a scanning electron microscope (SEM, Leo-Evo 40x VP). Incident electron beam energies from 3 to 30 keV had been used. In all cases, the beam was at normal incidence to the sample surface and the measurement time was 100 s. All the EDAX spectra were corrected by using the ZAF correction, which takes into account the influence of the matrix material on the obtained spectra.

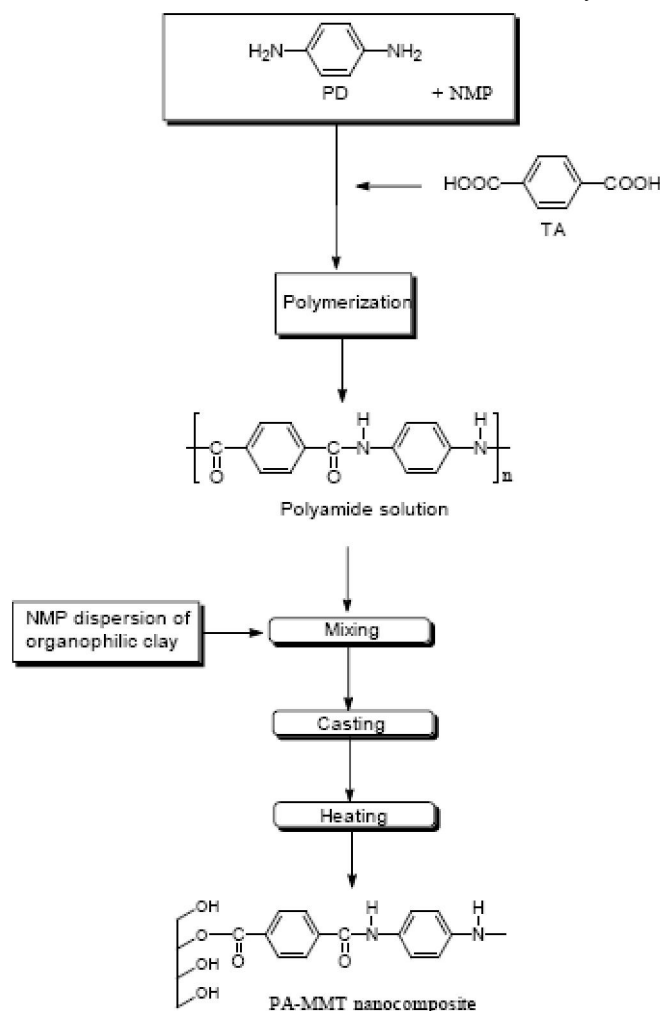
Dielectric constants were measured by Agilent Technologies 4294A Precision Impedance analyzer at 1-1000 kHz. The diameter of the electrode and the film was 20 mm. To ensure good electrical contact between the electrodes and the polyimide film, prior to measurement the films were sputter-coated for 20 s on both sides with a silver layer of around 0.05 μm . The dielectric constants of the film were determined over the frequency range of 100–107 Hz at room temperature.

Preparation of montmorillonite (MMT)

Natural montmorillonite clay from Resadiye region of Tokat, Turkey, was used in this work. The clay was obtained by the methods of dispersion and sedimentation and various chemical treatments applied to natural clay. The clay (20 g) was treated with of 100 ml of 10% $\text{CH}_3\text{SO}_3\text{H}$, methanesulfonic acid ($d = 1.48 \text{ g/ml}$, Sigma) solution for 4 h at 353 K, with slow agitation. It was further treated with 10% $\text{CH}_3\text{SO}_3\text{H}$ and 0.5 mol/dm³ potassium permanganate solution for 5 h at 353 K. Finally, it was washed with water until the neutral pH was obtained. The material dried in an oven at 353K for 24 h. Composition and specific surface area of the treated clay was found as: SiO_2 88%, Al_2O_3 5.2%, Fe_2O_3 2.7%, CaO 0.26%, MgO 0.17%, Na_2O 0.1%, K_2O 0.48%, MnO_2 0.08%; $\text{SBET} = 112.3 \text{ m}^2/\text{g}$.

Preparation of organically modified MMT

The organically modified MMT was prepared via ion exchange reaction in water using hexadecylpyridinium chloride. For the preparation of MMT modified with hexadecylpyridinium chloride



Scheme 1 : Synthesis of PA-MMT nanocomposite

(HPC), 1.0 g was mixed with 1 ml concentrated hydrochloric acid (37%) and 15 ml distilled water and heated at 80°C for a few minutes, and to it was added a dispersion of 2.5 g Na-MMT in 100 ml distilled water. The mixture was stirred vigorously for 1 h at 80°C. The white precipitate was filtered and washed repeatedly with hot water (80°C) to remove the superfluous hexadecylpyridinium chloride salts to be free from OM-MMT. It was subsequently collected and dried in vacuum at 80°C for 24 h.

Preparation of organically modified MMT-PA nanocomposites

A flask was charged with a mixture of *p*-phenylene diamine (1.12 mmol), terephthalic acid (0.18 g, 1.12 mmol), triphenyl phosphite (0.70 g, 2.24 mmol), pyridine (1 mL), NMP (5 mL), and 5 wt % LiCl. It was refluxed under N_2 overnight and poured into water. The

Full Paper

yellowish solid precipitate was filtered off, washed with water, and dried to afford PA (0.89 g, 95%). It was extracted with acetone in a Soxhled apparatus for 3h.

RESULTS AND DISCUSSION

Organo-modification of MMT

As previously mentioned, the organo-modification of MMT is an important step in the preparation of polymer-MMT nanocomposites and primary aliphatic amines such as 1-hexadecylamine and its quaternary ammonium salt were commonly used organic modifiers. IR and XRD were used to verify the organic modifiers designed by us have the same efficacy as the com-

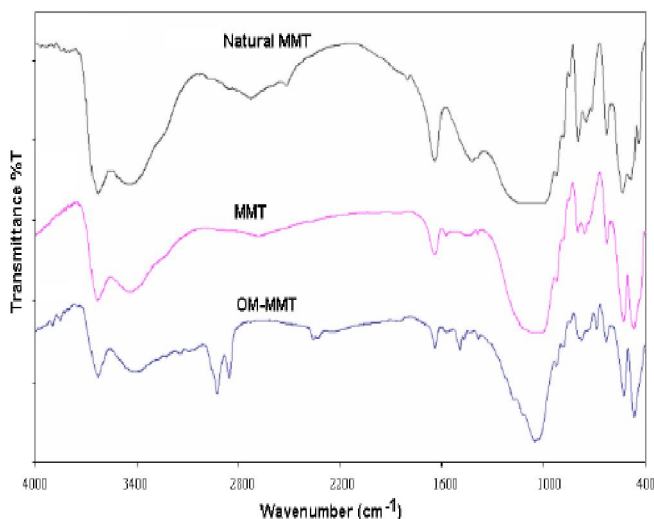


Figure 1 : The IR spectra of natural MMT, MMT, and OM-MMT.

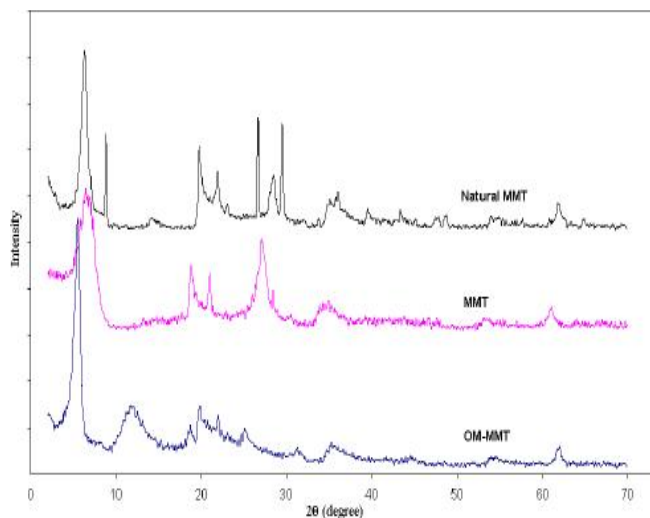


Figure 2 : The XRD patterns of Natural MMT, MMT, and OM-MMT.

monly used modifiers. Figure 1 is the IR spectra of natural MMT, MMT, and OM-MMT. The absorption bands at 1038 and 1090 cm^{-1} were characteristic of MMT (Figure 1). After the treatment, OM-MMT exhibited the characteristic bands of C–H stretching at 2914 and 2847 cm^{-1} .

The IR results only suggested that the treated MMT contained the organic modifiers but could not give the conclusion that the molecules of organo-modifiers entered the galleries of MMT. Figure 2 is the XRD patterns of Natural MMT, MMT, and OM-MMT. The interlayer spacing of MMT was obviously increased after the treatment with chloride salt of OM. This suggested that organo-modifiers synthesized by us successfully intercalated between layers of MMT. More importantly, it has been widely accepted that the basal spacing of MMT treated by long-chain aliphatic amine is decided largely by the chain length and long chain length leads to high d-value.

Thermal stability of organo-modified MMT

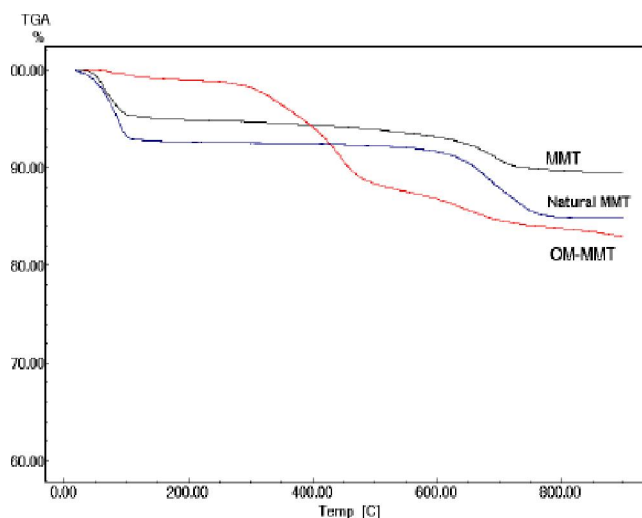


Figure 3 : The TGA curves of natural MMT, MMT and organo-modified MMT.

Figure 3 were the TGA curves of organo-modified MMT, which illustrated two or three-step degradation in the temperature range of 200–600 $^{\circ}\text{C}$. This phenomenon was also observed and studied by^[21] using DTA and MS. They proposed that the organics with a small molecular weight may be released first and those with a relatively high molecular weight may still exist between the interlayers until the temperature was high enough to lead to its further decomposition^[21]. The ini-

tial thermal decomposition temperature (onset temperature) of OM-MMT was 252°C. Natural MMT and MMT clearly showed higher initial thermal decomposition temperature compared to OM-MMT because of the higher thermal stability.

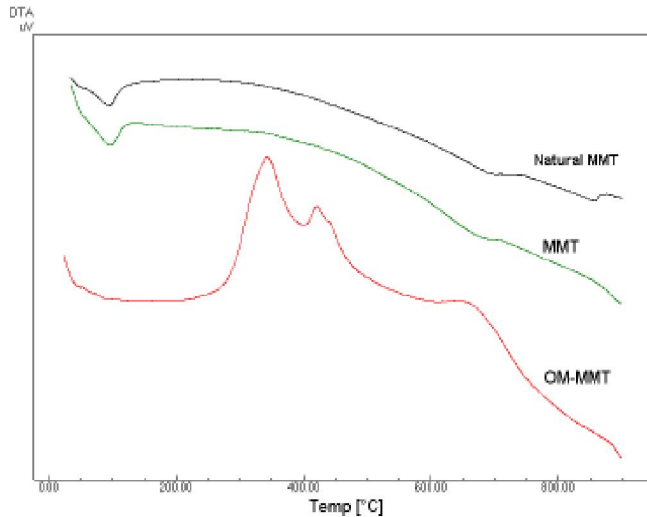


Figure 4 : The DTA curves of natural MMT, MMT and organo-modified MMT.

FTIR, XRD and SEM characterization of PA-MMT nanocomposite films

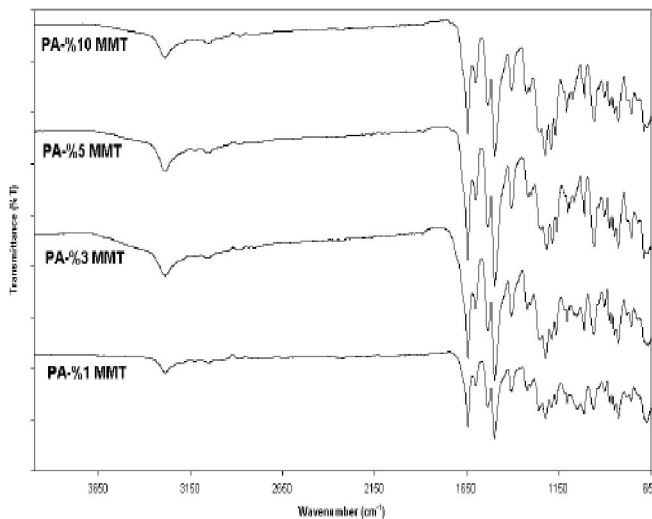


Figure 5 : FTIR spectra of the PA-MMT nanocomposite films

Figure 6 showed the XRD patterns of PA and PA-clay nanocomposite films. There was no peak below $2\theta = 10$ for the pure polyamide film and the PA-clay nanocomposite film of 1 wt% clay. Although the clay content was low (1 wt%), X-ray diffraction which is a powerful and sensitive technique to detect the ordered structure by diffraction angle revealed that the silicate

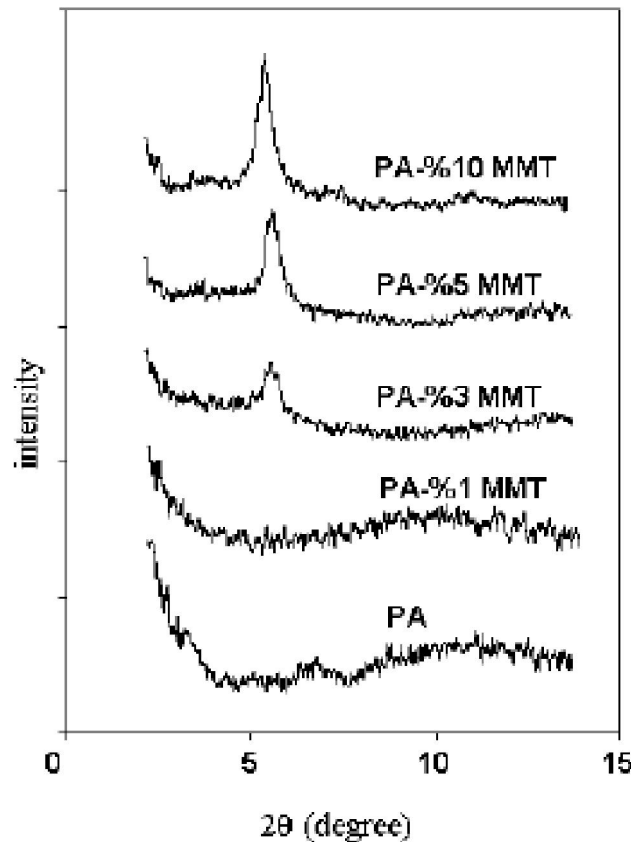


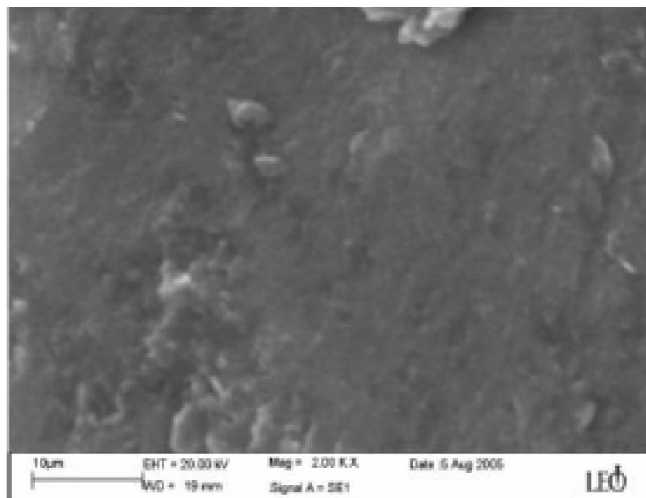
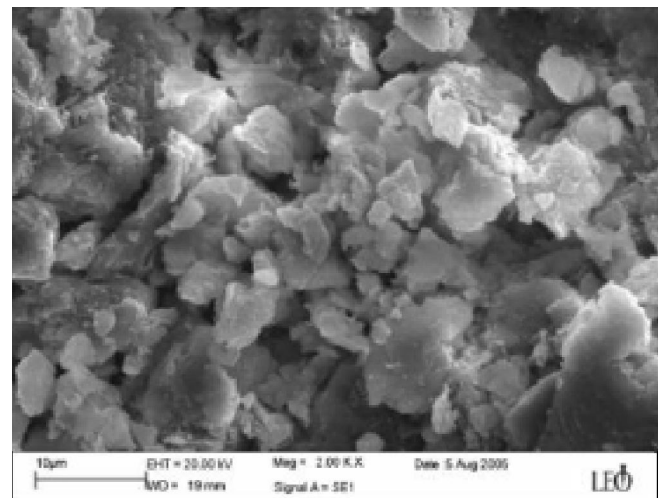
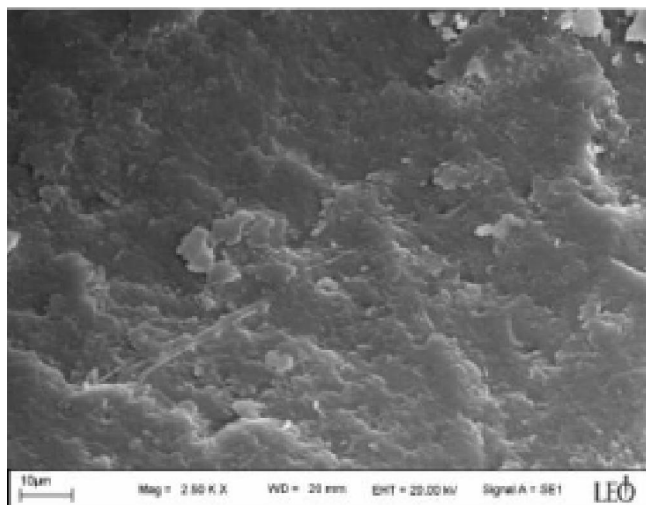
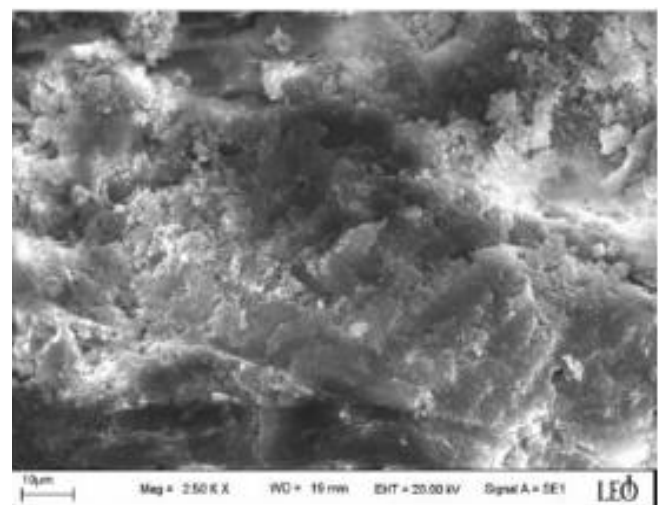
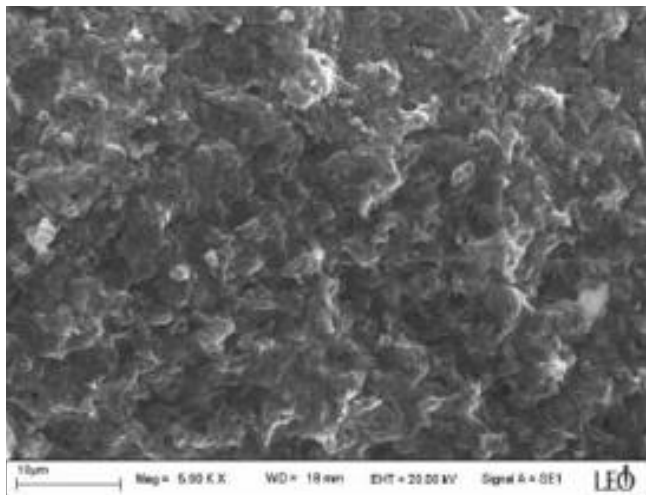
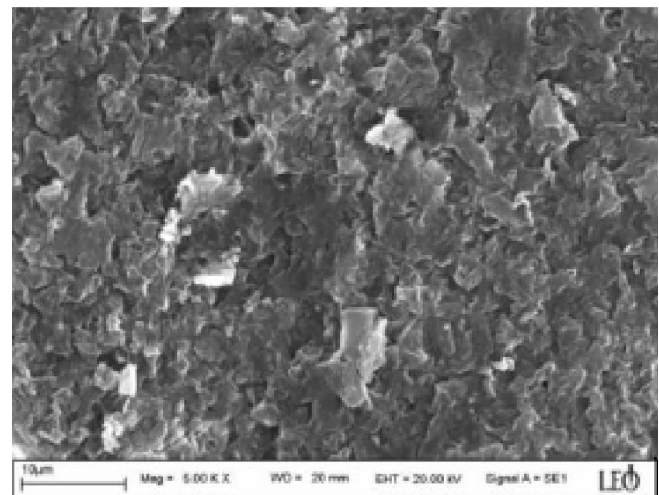
Figure 6 : The XRD patterns of PA and PA-MMT nanocomposite films

layers in PA-clay nanocomposite film of 1 wt% clay lost their ordered structure and were then separated. In other words, it could be regarded that the clay had been fully exfoliated and dispersed randomly in the polyamide matrix^[16, 17]. This could be confirmed by the SEM image shown in Figure 7. However, Pure PI had a relatively smooth fracture surface compared with those of hybrids with clays. At a clay content of 1 wt%, a rough morphology composed of numerous platelets orientated parallel to the film surface appeared over the entire fracture surface. At a clay content of 10wt%, much larger agglomerated clay particles were observed in the polymer hybrids.

Thermal properties of PA-MMT nanocomposites

Figure 8. TGA curves of PA-MMT nanocomposites with various MMT contents. (a: PA, b: PA-%1 MMT, c: PA-%3 MMT, d: PA-%5 MMT and e: PA-%10 MMT)

Figure 8 showed the TGA curves of PA-MMT nanocomposites with various MMT contents. The thermal stability of the nanocomposites was increased with

Full Paper**PA****OM-MMT****PA-1% MMT****PA-3% MMT****PA-5% MMT****PA-10% MMT****Figure 7 : SEM micrographs of fractured surfaces of images of the pure PA and PA-MMT nanocomposites.**

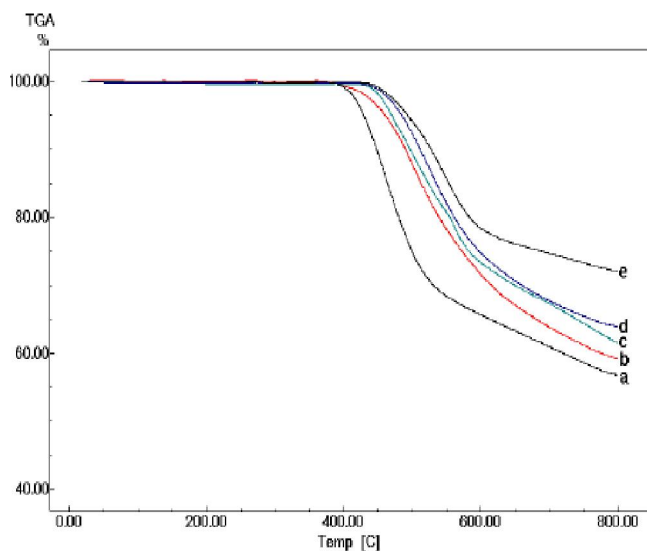


Figure 8 : TGA curves of PA-MMT nanocomposites with various MMT contents. (a: PA, b: PA-%1 MMT, c: PA-%3 MMT, d: PA-%5 MMT and e: PA-%10 MMT)

increased MMT content. The on-set thermal decomposition temperature accessed by TGA was increased from 522°C for PA to 550°C for PA-%1 MMT nanocomposite containing 1 wt% MMT. The on-set thermal decomposition temperature, temperatures at 5% and 10% weight loss were increased with the increase of MMT content. MMT possessed high thermal stability. Figure 9 showed the DSC curves of PA and PA-MMT nanocomposites with various MMT contents. The T_g of the nanocomposites was slightly increased as the MMT content was increased. The T_g was increased from 244°C for PA to 255°C for the

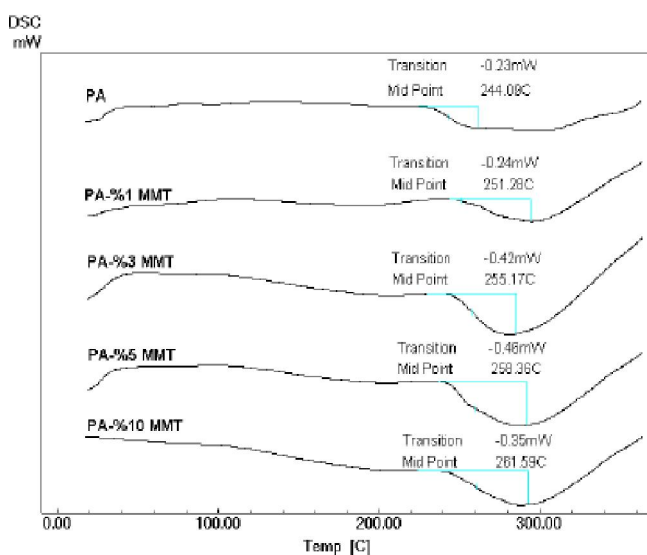


Figure 9 : DSC curves of the pure PA and the PA-MMT nanocomposites with various MMT contents

nanocomposite containing 3 wt% MMT and further to 261°C for the nanocomposite containing 10 wt% MMT. This could be due to the strong interaction between MMT and PA, which limited the cooperative motions of the PA chain segments.

Dielectric properties of PA– MMT nanocomposite films

Lower dielectric constant is one of the most desirable properties for next generation electronic devices. Dielectric constants of pure PA and PA-MMT nanocomposites with different MMT content are shown in TABLE 1 and Figure 10. The dielectric constant of the Nanocomposites decreases as the amount of clay is increased. The trend is the same as that in density^[28]. However, the dielectric constant of pure polyimide has relatively high values (3.8). The higher the density, the higher the dielectric constant in the polymer. The reduction in the dielectric constant of the PA–MMT nanocomposites can be explained a complicated polarization because of the special microstructure formed in the PA–clay nanocomposite films and term of creating the free volume increase by the presence of the rigid and large MMT structure resulting in a loose PI network. The density of the pure PA is 1.48 while the density of the PI-% 10 MMT is 1.14. PA is a semi-rigid polymer. A bigger MMT domain may increase slightly the separation of the PA interblock and increase the free volume and decrease the density. The void formation and the free volume increase of the PA-MMT nanocomposite can be qualitatively verified by its density. However, these results could be attributed to a complicated polarization because of the special microstructure formed in the PA–clay nanocomposite films. It is well know that the dielectric constant of a material is related to the polarization. When an alternating current (AC) is applied to the dielectric material, the complicated polarization could be initiated. Nevertheless, the microstructure of the PA–clay nanocomposites would have an influence on the polarization behavior. It can be explained that the interface polarization influenced the dielectric constant of the PA–clay nanocomposites with 1 wt% clay, as a significant amount of two-phase interfaces were formed between the exfoliated/ intercalated clay and polyamide matrix. However, the dispersion of clay would gradually changed from partially intercalated

Full Paper

and partially aggregated (3 wt%) to severely aggregated (5 and 10 wt%). The dispersion of clay with multilayer structure was confirmed by the XRD (Figure 6), transparency and mechanical properties of the films^[29-31].

TABLE 1 : Density and dielectric properties of pure polyamide (PA) and PA-MMT composites.

Sample	Dielectric constant (k) ^a	Dielectric constant (k) ^b	measured density (g/cm ³)
PA	3.81	3.50	1,48
PA-%1 MMT	3.40	3.17	1,32
PA-%3 MMT	3.27	3.09	1,28
PA-%5 MMT	3.09	2.91	1,21
PA-%10 MMT	3.05	2.61	1,18

^aDielectric constant measured by LCR meter at 1 MHz.

^bDielectric constant measured by LCR meter at 10 MHz.

Therefore, the dielectric constant of PA–clay films with the clay content more than 3 wt% was lower than those of the pure PA and PA–clay film with 1 wt% clay. Furthermore, As shown in these Figures, the dielectric constant was insensitive to the frequency except at the very low frequency where the dielectric constant was slightly higher. The dielectric constant of PA–clay nanocomposite film with 1 wt% was higher than that of pure PA film at the whole experimental frequency range.

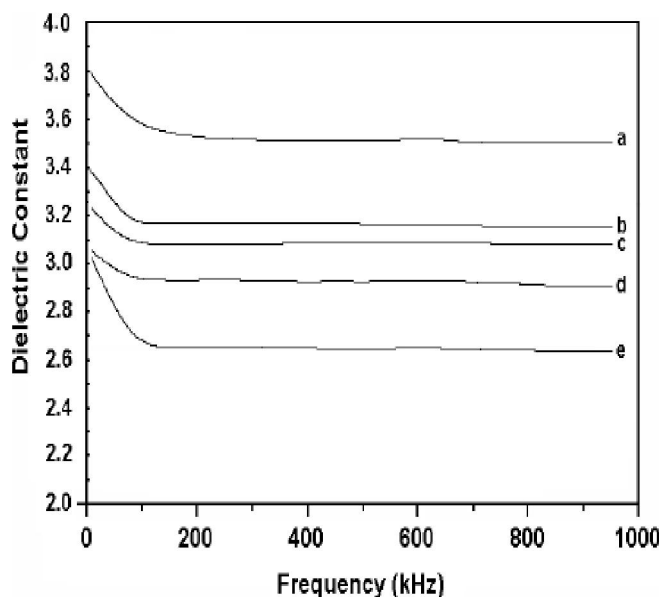


Figure 10. dielectric constants of pure polyamide (a) and PA-MMT composites (b: PA-%1 MMT, c: PA-%3 MMT, d: PA-%5 MMT and e: PA-%10 MMT)

CONCLUSIONS

In this study, the structure of polyamide and polyamide–clay films prepared via intercalation process from *p*-phenylenediamine (PD), terephthalic acid (TA) and organo-clay has been characterized using XRD and TEM techniques. The dielectric and thermal properties of the PA–clay nanocomposite films were studied in detail. The results displayed that the dielectric constants decreased with the increase of the clay content and the films showed relatively low dielectric constant when the clay content was over 1 wt% compared to pure polyamide. In general, the polyamide–clay nanocomposite films also displayed relatively low dielectric loss, higher storage modulus and high glass transition temperature. Therefore, PA–clay nanocomposite films are potential advanced dielectric materials which could be suitable for being employed in the microelectronic and cryogenic engineering applications.

REFERENCES

- [1] S.Russo, E.Bianchi, A.Congiu, A.Mariani, R.Mendichi; *Macromolecules*, **33**, 4390-4397 (2000).
- [2] J.Wang, R.Nomura, T.Endo; *Journal of Polymer Science Part A: Polymer Chemistry*, **35**, 1381-1387 (1997).
- [3] Y.H.Kim, J.C.Calabrese; *Macromolecules*, **24**, 2951-2954 (1991).
- [4] J.Wang, R.Nomura, T.Endo; *J.Polym.Sci.Part.A.Polym.Chem.*, **33**, 2901-2908 (1995).
- [5] P.E.Cassidy; *Thermally Stable Polymers*, Marcel Dekker, New York, (1980).
- [6] H.H.Yang; *Aromatic High Strength Fibres*, Wiley and Sons, New York, (1989).
- [7] D.Adame, G.W.Beall; *Applied Clay Science*, **42(3-4)**, 545-552 (2009).
- [8] S.Zulfiqar, M.Ishaq, M.I.Sarwar; *Surface and Interface Analysis*, **40(8)**, 1195-1201 (2008).
- [9] L.Tianxi, P.L.Kian; *Polymer*, **44**, 3529-3535 (2003).
- [10] M.Zanetti, G.Camino; *Polymer*, **42**, 4501-4507 (2001).
- [11] B.Alexandrea, S.Maraisa, D.Langevina, P.Mederich, T.Aubry; *Desalination*, **199**, 164-166 (2006).

- [12] J.Y.Jadhav, J.Preston, W.R.Krigbaum; J.Polym.Sci.Part A.Polym.Chem., **27**, 1175-1195.
- [13] P.B.Messersmith, E.P.Gianelis; J.Polym.Sci.A.Polym.Chem., **33**, 1047-1057 (1995).
- [14] R.Scaffaro, M.C.Mistretta, F.P.La Mantia; Polymer Degradatýon And Stabýlýty, **93(7)**, 1267-1274 (2008).
- [15] Y.J.Li, Y.Iwakura, H.Shimizu; Journal of Nanoscýence and Nanotechnology, **8(4)**, 1714-1720 (2008).
- [16] L.Mezzaros, T.Czvikovszky; Radýatýon Physýcs and Chemýstry, **76(8-9)**, 1329-1332 (2007).
- [17] S.Mohanty, S.K.Nayak; Polymer Composýtes, **28(2)**, 153-162 (2007).
- [18] P.M.Gyoo, S.Venkataramani, S.C.Kim; Journal of Applýed Polymer Scýence, **101(3)**, 1711-1722 (2006).
- [19] B.Gupta, M.F.Lacrampe, P.Krawczak; Polymers & Polymer Composýtes, **14(1)**, 13-38 (2006).
- [20] A.Usuki, M.Kawasumi, Y.Kojima, A.Okada, T.Kurauchi; J.Mater.Res., **8**, 1174-1184 (1993).
- [21] W.Xie, Z.Gao, K.Liu; Thermochim Acta., **367-368**, 339-350 (2001).
- [22] Y.Kojima, A.Usuki, M.Kawasumi, A.Okada, Y.Fukushima, T.Karauchi; J.Mater.Res., **8**, 1185-1189 (1993).
- [23] K.G.Fournaris, M.A.Karakassides, D.Petridis; Chem Mater., **11**, 2372-2381 (1999).
- [24] B.K.Theng; Formation and Properties of Clay-Polymer Complexes, Elsevier, Amsterdam, (1979).
- [25] T.Lan, T.Pinnavaia; Chemýstry of Materýals, **6**, 2216-2219 (1994).
- [26] T.Seckin , S.Koytepe , N.Kivilcim , E.Bahce, I.Adiguzel; Journal of Polymerýc Materýals, **57**, 429-441 (2008).
- [27] E.D.Giannelis; Adv.Mater., **8**, 29-35 (1996).
- [28] S.J.Kang, D.J.Kim, J.H.Lee, S.K.Choi, H.K.Kin; Mol.Cryst.Liq.Cryst., **280**, 277-282 (1996).
- [29] C.M.Leu, Y.T.Chang, K.H.Wei; Macromolecules, **36**, 9122-9127 (2003).
- [30] Y.J.Leea, J.M.Huangb, S.W.Kuoa, J.S.Lua, F.C.Changa; Polymer, **46**, 173-181 (2005).
- [31] M.H.Tsai, W.T.Whang; Polymer, **42**, 4197-4207 (2001).